A Rapid and Simple Method for Determination of Uranium in Gattar Area by ICP-OES

El-Wakil, A.F. and Mahdy, N.M.

E.mail:azzafw@yahoo.com

ABSTRACT

This experiment was carried out to determine Uranium in a geological samples collected from Gattar area, North Eastern Desert of Egypt which examined by scanning electron microscope (EDX) to be characterized by hematization, silicification, muscovitization and fluoritization which are the most dominant alteration associated with the uranium mineralization. Inductively coupled plasma optical emission spectrometry (ICP-OES) was used for this study. Two methods of digestion of samples were used in the experiment and four emission lines were selected for uranium to choose the more sensitive one. The physical parameter conditions were adjusted by using standard solution of uranium to be 1200 W for RF power current, 35 psi for nebulizer gas pressure and 18 L/min for coolant gas pressure. The interference effect of some elements was studied on the selected line and showed that, the determination of uranium by ICP-OES is affected seriously by iron, aluminum, calcium, thorium and rare earth elements. The results of uranium determination at 303.199 nm with precipitation method were compared with the results from XRF method which shown acceptable accuracy and low time consuming other method.

1.   Nuclear Materials Authority, P. O. Box 530 El Maadi, Cairo, Egypt.

.INTRODUCTION

Uranium occurs naturally in low concentration in rock and soil; it decays slowly by emitting (α) particles. Uranium and its compounds are very important especially during the processing of nuclear fuel. Therefore the development of an accurate analytical method for uranium determination is always important **(Reddy et al., 2011)**.

Sensitive and reliable analytical method for the determination of Uranium is very important for the evaluation in geological samples. Various methods have been used for this purpose including atomic absorption spectrometry **(Anirudhan et al., 2010)**, molecular absorption spectrometry **(Ferreira et al., 2006)**, fluorimetry **(Tarafder et al., 2002)**, inductively coupled plasma mass spectrometry **(grinberg et al., 2005)** and X-ray fluorescence **(Rathore, 2008)**.

Inductively coupled plasma optical emission spectrometry (ICP-OES) is widely used for the determination of elements in different materials as water, soil and geological materials **(Florian et al., 1998 and Marin et al., 2008)**.

The ICP-OES system may suffers from some errors originated from the measurement techniques or from different steps before the analytical procedure which must take care of it such as collecting, storage and sample preparation

The Uranium determination by ICP-OES has difficulties that limit the accuracy and precision of the obtained data. Uranium has several spectral lines in the wavelength range between 200 nm and 400 nm. So, it is very important for accurate determination is the line which must be free of element interference. If the sample contains interfering elements with line – rich spectra, the detection power could be lost. The main reasons are the partial or complete between the analytic lines and the concomitants lines, a higher noise and a decrease of the signal to background ratio **(Avranov et al., 2009)**.

MATERIALS AND METHOD

Instrumentation and operating conditions

Measurements were performed using Prism ICP high dispersion, Teledyne Leeman Labs. (U.S.A.) with an axial configuration whose operating conditions in Table (1) and JENWAY pH meter was used to determine the pH balance of the samples.

Table (1) : *The operating conditions of ICP-OES.*

Parameter	Plasma conditions
RF power current	1200 Watt
Coolant gas	18 ml/min
Nebulizer gas flow	35 psi
Sample uptake rate	1.4 ml/min
Sample uptake time	20 sec
Replicates	3
PMT voltage	800 V

Reagents and Materials

All acids were of the grade for inductively coupled plasma (Burdick& Jackson, Germany), the standards used for calibration and overview of the physical operating parameters were ICP-AES & ICP-MS and ICP-OES standard solutions 1000 ppm spikes on 4% HNO_3 manufactured in Canada. High-purity water with a resistivity >18MΩ was obtained from Human lab Instrument Co. and fed with de-ionized water (Aquatron).

RESULTS AND DISCUSSION

In this study, the lines U286.568, U302.221, U303.199 and U306.254 were chosen with the consideration of the least spectral interference with uranium. To obtain the most accurate line for the determination of uranium in some geological samples, two standard solutions of uranium with concentration 6.3×10^{-5} and 10.5×10^{-5} M (single element) was used to test the lines and obtain the correct determination one with acceptable accuracy, table 2 showed that, the line 303.199 nm was relatively the most accurate line, which has a linear calibration curve ($r^2 =0.997$) in the range from 4.2×10^{-6} M (1ppm) to 42.0×10^{-6} M (10ppm) with detection limit up to 0.21×10^{-6} M (50 ppb) . The standard solution of 10.5×10^{-5} M uranium was used also to evaluate the effect of some physical parameters on the accuracy of the determination using the selected line. For studying the effect of the radio frequency power, the power range between 600W and 1400W was studied (table 3-a) to obtain the optimum reading at 1200 W. While in case of the effect of the coolant gas pressure, the studied range was between 14 and 20L/min using standard solution of uranium with conc. 10.5×10^{-5}M (table 3-b). For the nebulizer gas pressure which controls the sample exposure with plasma, this parameter was studied by the same standard solution of uranium in the range between 20 and 45 Psi. to give the optimum readings at 35 Psi respectively (table 3-c).

Table (2) : *The selection of the most accurate line of uranium relative to two concentrations.*

Wave length (nm)	Actual conc. Of Uranium (M)	Measured conc. Of Uranium (M)	SD (σ)	RSD (%)	Accuracy (%)	Uncertainty (u)
286.568 nm	6.3×10^{-5} M	0.5×10^{-5} M	0.06245	12.49%	7.94%	0.0361
	10.5×10^{-5} M	1.99×10^{-5}M	0.09539	4.79%	18.95%	0.0551
302.221 nm	6.3×10^{-5} M	2.35×10^{-5} M	0.11358	4.83%	37.30%	0.0656
	10.5×10^{-5} M	4.32×10^{-5}M	0.070	1.62%	41.14%	0.0404
303.199 nm	6.3×10^{-5} M	7.15×10^{-5} M	0.03606	0.50%	86.51%	0.0208
	10.5×10^{-5} M	12.71×10^{-5}M	0.030	0.24%	78.95%	0.0173
306.254 nm	6.3×10^{-5} M	1.11×10^{-5}M	0.02646	2.38%	17.62%	0.0153
	10.5×10^{-5} M	2.14×10^{-5}M	0.030	1.40%	20.38%	0.0173

Table (3)a : *The effect of RF power current on the accuracy % of the uranium determination at wavelength 303.199 nm.*

RF power current	600 W	800 W	1000 W	1200 W	1400 W
Actual U con.	10.5×10^{-5} M	10.5×10^{-5} M	10.5×10^{-5} M	10.5×10^{-5} M	10.5×10^{-5} M
Measured U conc.	4.2×10^{-5} M	5.7×10^{-5} M	6.8×10^{-5} M	10.0×10^{-5} M	12.9×10^{-5}M
SD (σ)	0.06245	0.08888	0.10066	0.1044	0.08888
RSD (%)	1.49%	1.56%	1.48%	1.04%	0.69%
Accuracy (%)	40%	54.29%	64.76%	95.24%	77.14%
Uncertainty (u)	0.0361	0.0513	0.0581	0.0603	0.0513

Table (3)b : *The effect of coolant gas pressure on the accuracy % of the uranium determination at wave length 303.199 nm.*

Coolant gas pressure	14 L/min.	16 L/min.	18 L/min.	20 L/min.
Actual U con.	10.5×10^{-5} M	10.5×10^{-5} M	10.5×10^{-5} M	10.5×10^{-5} M
Measured U conc.	5.2×10^{-5} M	7.4×10^{-5} M	10.1×10^{-5} M	12.2×10^{-5} M
SD (σ)	0.02646	0.03605	0.30	0.06557
RSD (%)	0.51%	0.49%	0.30%	0.54%
Accuracy (%)	49.52%	70.48%	96.19%	83.81%
Uncertainty (u)	0.0153	0.0208	0.1732	0.0379

Table (3)c : *The effect of nebulizer gas pressure on the accuracy % of the uranium determination at wave length 303.199 nm.*

Nebulizer gas pressure	20 Psi	25 Psi	30 Psi	35 Psi	40 Psi	45 Psi
Actual U con.	10.5×10^{-5} M	10.5×10^{-5} M	10.5×10^{-5} M	10.5×10^{-5} M	10.5×10^{-5} M	10.5×10^{-5} M
Measured U conc.	5.9×10^{-5} M	7.3×10^{-5} M	8.5×10^{-5} M	10.6×10^{-5} M	11.8×10^{-5}M	13.7×10^{-5} M
SD (σ)	0.0264	0.02646	0.04582	0.02646	0.02645	0.030
RSD (%)	0.45%	0.36%	0.54%	0.25%	0.22%	0.22%
Accuracy %	56.19%	69.52%	80.95%	99.05%	87.62%	69.52%
Uncertainty (u)	0.0152	0.0153	0.0265	0.0153	0.0153	0.0173

An important part of the detection power of ICP-OES could be lost if the sample contains a major element with line-rich spectra so, the interference effect of some elements was studied on the selected line using a solution of 8.4×10^{-5} M uranium with the expected interfering elements which showed that, the determination of uranium by ICP-OES is affected seriously by iron, aluminum, calcium, thorium and rare earth elements (table 4). Accordingly, pre-concentration and separation procedure is required to overcome the interferences caused by the interfering metals which will be by precipitation in this study. The separation and determination process were applied on a granitic samples from Gattar, North Eastern Desert, Egypt.

Table (4) : *The interference effect of some metals on the determination of 8.4×10^{-5} M standard solution uranium.*

8.4×10^{-5} M standard solution of U at wavelength 303.199 nm									
(Fe) effect		**(Al) effect**		**(Ca) effect**		**(Th) effect**		**(Total REEs)effect**	
Added (Fe) conc. $\times 10^{-4}$ M	Measured U $\times 10^{-5}$M	Added (Al) conc. $\times 10^{-3}$ M	Measured U $\times 10^{-5}$M	Added (Ca) conc. $\times 10^{-4}$ M	Measured U $\times 10^{-5}$M	Added (Th) conc. $\times 10^{-5}$ M	Measured U $\times 10^{-5}$M	Added (REEs) conc. $\times 10^{-6}$ M	Measured U $\times 10^{-5}$M
17.54	33.7	3.7	16.8	12.5	14.1	4.3	7.6	2.28	8.07
35.09	40.9	7.4	30.4	25.0	21.4	8.6	6.6	4.56	7.98
52.63	46.6	11.1	41.9	37.5	28.5	12.9	5.4	6.84	7.81
70.18	56.6	14.8	68.0	50.0	34.2	17.2	4.4	9.11	7.61
87.72	109.7	18.5	87.9	62.5	40.3	21.6	4.1	11.39	7.27

Geological Setting and Sample Description

Gattar batholith outcrops over an area of ca. 450 km^2 in the north Eastern Desert of Egypt. Gattar batholith defines roughly elongated and elliptical shape, and extends N-S for about 33 Km and E-W for about 20 Km (Figure 1). It is composed of mountainous terrains with higher topographic elevations if compared to the surroundings (G. Gattar, G. Um Dissi, G. Khela, G. Abu El Hassan, G. Abu El Hassan El Ahmar, G. Um Samyuki and G. Ain Ruyashed). Along W. El Ghoza, the batholith is clearly classified into different parts (Red and Pink granite). The country rocks (Figure 1) include huge bodies of metavolcanics, arc granitoids and Hammamat sedimentary rocks (molasse-type sediments).

The uranium mineralization occurs at the northern part of the batholith at its periphery with Hammamat sedimentary rocks (Figure 1). The uranium mineralization is hosted by Gattar red granite (alkali-feldspar granite) within altered fractured and sheared zones of the granite. In other terms, the uranium mineralization is structurally controlled (the fractures, joints and sheared zones represent structural traps of this mineralization). The ore deposits are associated with the conjugated fault system (Figures 1 and 2) **(Mahdy, 2011; Mahdy *et al*., 2014 and Mahdy *et al*., 2015)**. The uranium mineralization is hydrothermally produced and associated with alterations of the host Gattar granite. The size of hydrothermal minerals increases with degree of alteration, and the alteration displays vast zonings close to the U mineralization, mainly characterized by hematitization, silicification, muscovitization and fluoritization but the hematitization, silicification, and fluoritization are the most dominant alteration associated with the U mineralization (Figure 2).

The iron oxides occur as fillings (cavities and vugs), and coatings within the granite along the fractures and joints (Figures 1b and 2a). Within high-grade U deposits, the degree of hematitization increases. The hematitized granites are hard and their colors become reddish brown to brown due to the impregnation of all forming minerals with hematite and loss of their plagioclase and perthite contents.

Silicification is a common alteration feature within the U mineralized zones. It is commonly represented by white and smoky quartz veinlets filling joints, fractures and shear zones that are dominant through the NNE-SSW, NW-SE and E-W trends (Figure 1a, c). Quartz occurs as primary crystals of medium size and as secondary fine crystals filling the interstices between the minerals. It shows five forms **(Mahdy, 2011)**:

1. Crushed grains occupying the inter-granular spaces between the other essential minerals,

2. Inclusions of variable sizes and shapes within the other mineral phases,

3. Inclusions of fine rounded grains inside and at the edges of feldspar crystals forming poiklitic texture, i.e., si1icification processes,

4. Overgrowth as result of dissolution of quartz, and

5. Relics of magmatic quartz surrounded by automorphic euhedral quartz and this type rise from the recurrent dissolution-recrystallization of quartz.
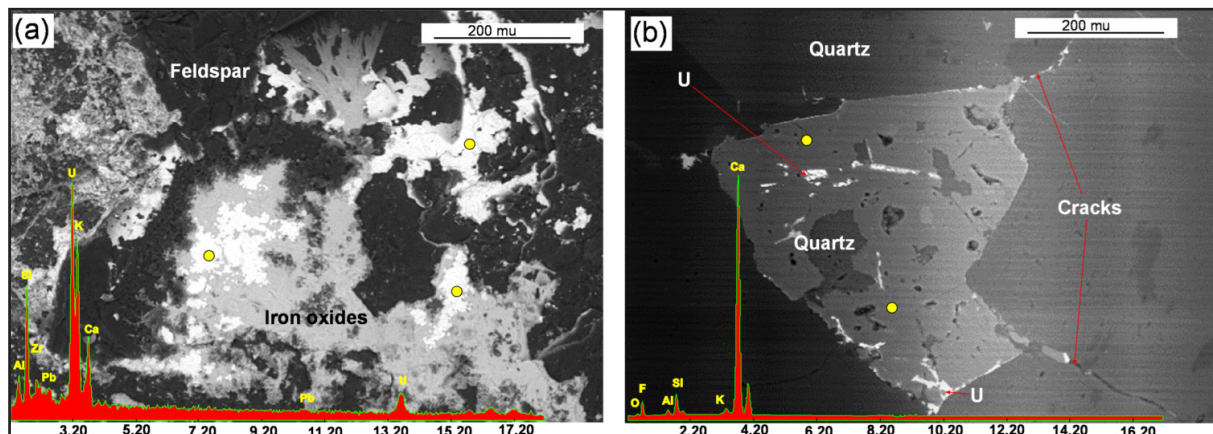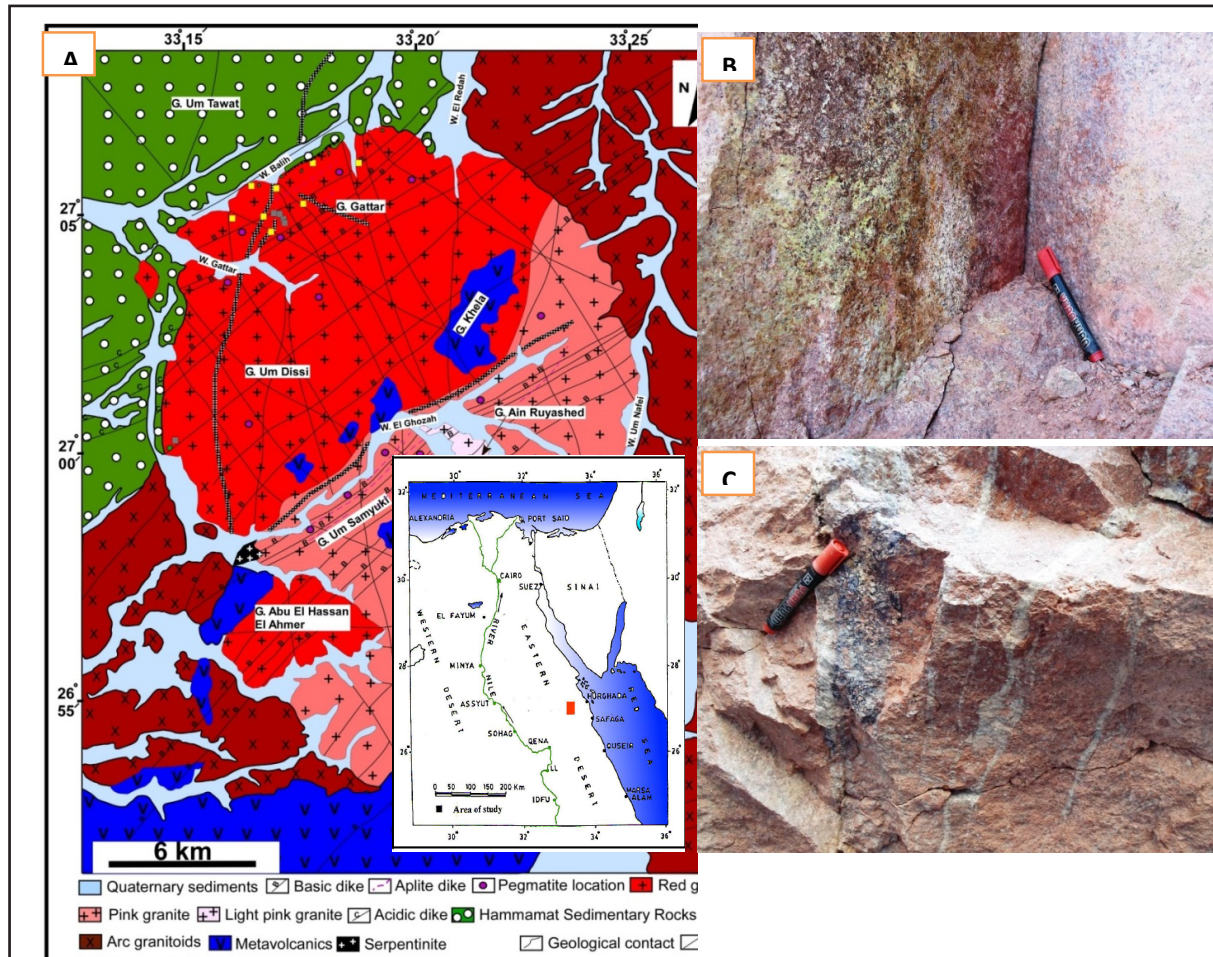
Fluoritization is an important alteration feature associated with the U mineralization (Figures 1b and 2b). Fluorite occurs as disseminations and / or forming thin veinlets and encrustations filling some mineralized fissure and fractures. Fluorite is mostly characterized by its dark violet color as result of exogenic of uranium breakdown and evolution of hydrothermal solutions (Figure 1c) *(Mahdy et al., 2014 and Mahdy et al., 2015)*.

Figure (1)**:** (a) Geological map of the Gattar batholith showing the structure framework affected the area, rock units, and locations of U-Mo mineralized zones of Gattar granite as occurred at the north-

ern part of the batholith and close to Hammamat sedimentary rocks after **Mahdy et al., (2015)**. Field photographs (b and c) showing that the yellow visible secondary uranium is associated with intensive hematitization and silicification (b). The dark violet fluorite and quartz veins are mainly associated with the uranium deposits in the Gattar granite (c).

Figure (2): Backscattered electron (BSE) images

Legend		
Quaternary sediments	Basic dike	Aplite dike · Pegmatite location ▮ Red g
Pink granite	Light pink granite	Acidic dike Hammamat Sedimentary Rocks
Arc granitoids	Metavolcanics Serpentinite	Geological contact

and scanning electron microscope (EDX) spectrums showing that the uranium mineralization of Gattar granite is intimately associated with iron oxides, and EDX pattern exhibiting uranophane or Beta-uranophane phases (illuminated bright colors) as the main uranium phases of uranium deposits in Gattar granite (a). The fluorite mineral (identified by EDX) encloses the uranium minerals as inclusions and is associated with quartz; the cracks in quartz indicate that the fluorite and uranium may be formed as post-magmatic phases after fracturing of the Gattar granite (b). Note: yellow spots refer to the spot analyses measured by scanning electron microscope.

Separation and Determination

The granitic samples were digested by two methods:

1- Excess HF with heating till dryness, cooling and adding HF (1:1), filter and to measure U in the filtrate (solution 1)

2- 10 ml of 40%HF, 5 ml of 68%HNO$_3$ and 5 ml of 20%HClO$_4$ till complete drying and dissolves in 15 ml of 20% HCl. (solution 2)

Few drops of concentrated nitric acid (68%) were added to solution (2) and then boiled to convert iron (II) to iron (III).

$$3Fe^{2+} + NO_3^- + 4H^+ = 3Fe^{3+} + NO + 2H_2O$$

0.2 g of ammonium chloride was added and ammonium hydroxide solution was used to precipitate mainly iron and aluminium (M^{3+}) as hydroxides at pH 9. By filtration and washing the precipitate with 1% ammonium chloride solution, the main interfering elements were separated from uranium. The precipitate was dried at 60°c for 2 hours and scanned by scanning electron microscope (Nuclear Materials Authority, Egypt) (Figures 3,4) which showed the one sample before and after separation.

The filtrates of solution (1) and the filtrate of solution (2) after precipitation were measured by ICP-OES at the line 303.199 nm and the obtained results compared with the results of the same samples measured at XRF technique (Nuclear Materials Authority, Egypt) which showed that, the determination after precipitation (2) is the closest result and has acceptable accuracy % comparing with other technique (table 5).On the other hand the studied method was applicated on two international standard references OKA-2 and BL-4a to validate the method (table 6).
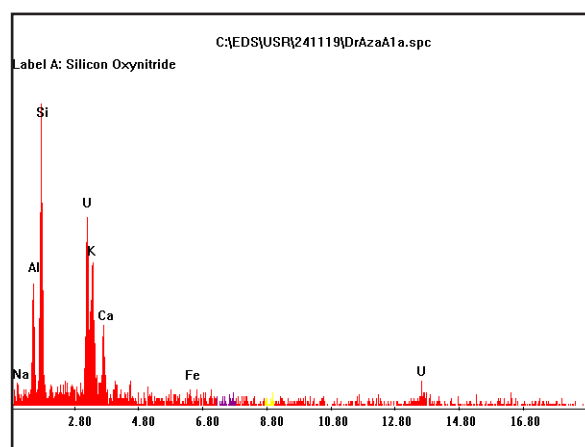

Fig. (3): The scan of the original sample which shows the existence of uranium with iron, aluminium, alkali metals and silicon.
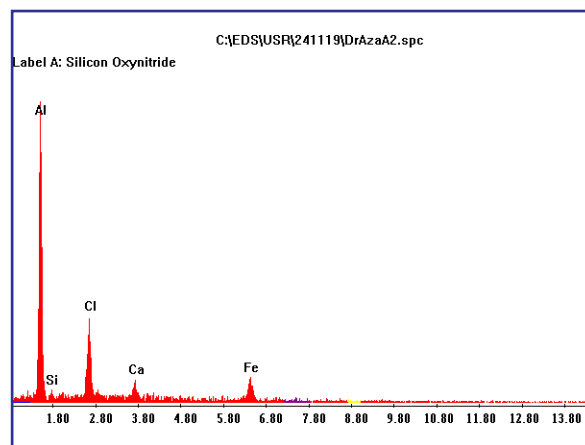

Fig. (4): The scan of the precipitate which shows the separation of uranium.

Table (5) : *Comparison between the measured uranium concentrations in granitic rock samples using ICP-OES and XRF.*

| Expected conc. by XRF × 10⁻⁴ M | Measured conc. By ICP-OES | | | | | | | |
| | By precipitation | | | | By excess HF | | | |
	Conc.×10⁴ M	RSD %	Accuracy%	Uncertainty	Conc.×10⁴ M	RSD%	Accuracy%	Uncertainty
45.59	42.35	0.10%	92.893%	0.0253	14.55	0.24%	31.915%	0.020
46.05	43.07	0.10%	93.529%	0.030	22.13	0.12%	48.056%	0.020
92.24	90.00	0.14%	97.572%	0.080	43.84	0.06%	47.528%	0.020

Table (6) : *Comparison of uranium concentration in international standard references and the present studied method.*

International Standard References	Certified value (M)	Measured U conc.(M)	SD (σ)	RSD%	Accuracy%	Uncertainty (u)
OKA-2*	91.85 × 10⁻⁵M	88.34 × 10⁻⁵ M	0.02000	0.02%	96.1786%	0.0200
BL-4a*	52.24 × 10⁻⁴M	50.87 × 10⁻⁴ M	0.04359	0.09%	97.3775%	0.0522

Certified values reported by Canadian Central for Mineral and Energy Technology standard (CANMET), certifying agency.

CONCLUSION

In this study, ICP-OES (at Nuclear Materials Authority, Cairo, Egypt) was used for uranium determination without a prior separation with traditional techniques as solvent extraction or resin. In this work, the physical parameters of the instrument were optimized for the selected uranium wavelength, the interference effect from the contaminant elements were examined. The Applied geological samples from North Eastern Desert of Egypt was digested and precipitated using ammonium chloride and ammonium hydroxide to eliminate M^{3+} interfering elements, uranium by present study was measured and compared with the result obtained from XRF technique, this method use cheap and available chemicals and not consume time.

REFERENCES

- **Anirudhan, T.S. and S.S. Sreekumari, S.S. (2010):** Synthesis and characterization of a functionalized graft copolymer of densified cellulose for the extraction of uranium (VI) from aqueous solutions. Colloids. Surf. A Physicochem. *Eng. Asp.*, 361(1-3): 180.

- **Avranov, M.; Cobos, J.; Popa, K. and Rondinella, V.V. (2009):** Determination of REE, U, TH, Ba and Zr in simulated hydrogeological leachates by ICP-AES after matrix solvent extraction. *J. Rare Earths.*, 27(1): 123.

- **Ferreira, H.S.; Benzerra, M.D. and Ferreira, S.L.C. (2006):** A pre-concentration procedure using cloud point extraction for the determination of uranium in natural water. *Microchem. Acta.*, 154 (1-2): 163.

- **Florian, D.; Barnes, R.M. and knapp, G. (1998):** Comparison of microwave assisted acid leaching techniques for the determination of heavy metals in sediments, soils and sludges. *J. Anal. Chem.*, 362(7-8): 558.

- **Grinberg, P.; Willie, S. and Sturgeon, R.E. (2005):** Determination of U, Th and Pu in natural waters. Biological materials and clinical samples by ETV-ICP-MS. *J. Anal. At. Spectrom.*, 20: 717.

- **Mahdy, N.M. (2011):** Mineralogical Studies and Mineral Chemistry of Some Radioactive Mineralizations in Gabal Gattar Area, Northern Eastern Desert, Egypt. MSc thesis. Ain Shams University.

- **Mahdy, N.M.; Shalaby, M.H.; Helmy, H.M.; Osman, A.F.; El Sawey, E.H. and Abu Zeid, E.K. (2014):** Trace and REE element geochemistry of fluorite and its relation to uranium mineralizations, Gabal Gattar Area, Northern Eastern Desert, *Egypt. Arab. J. Geosci.*, 7: 2537-.

- **Mahdy, N.M.; El Kalioubi, B.A.; Wohlgemuth-Ueberwasser C.C.; Shalaby, M.H. and El-Afandy, A.H. (2015):** Petrogenesis of U- and Mo-bearing A2-type granite of the Gattar batholith in the Arabian Nubian Shield, Northeastern Desert, Egypt: Evidence for the favorability of host rocks for the origin of associated ore deposits. Ore Geology Reviews, 71: 57.

- **Marin, B.; Chopin, E.I.B.; Jupinet, B. and Gauthier, D. (2008):** Comparison of microwave assisted digestion procedures for total trace elements content determination in calcareous soils. *Talanta.*, 77(1): 282.

- **Rathore, D.P.S. (2008):** Advances in technologies for the measurement of uranium in diverse matrices. *Talanta.*, 77(1): 9.

- **Reddy, G.C.; Devanna, N. and Chandrasekhar, K.B. (2011):** Derivative spectrophotometric determination of uranium (VI) using diacetylmonoxime isonicotinoyl hydrazone (DMIH). *Orbital Elec. J. Chem., Campo Grande*, 3(1): 24.

- **Tarafder, P.K.; Murugan, P.; Kunkal, L. and Rathore, D.P.S. (2002):** Extraction of uranium with 2, 3- Dihydroxynaphthalene and Cetyltrimethyl ammonium bromide and its fluorimetric determination in silicate rocks. *J. Radio Anal. Nucl. Chem.*, 253(1): 135.